Safety Moment

Global Warming Making Spring Allergies Bloom Earlier

RESEARCHERS SAY GLOBAL WARMING IS LEADING TO LARGER PLANTS AND EARLIER AND STRONGER POLLINATION

What You Can Do

Start early on allergy medication – trees may bud early, so **don't wait to take medicine**

Take antihistamines at night – their effectiveness peaks in the morning

Nasal washes are a natural alternative - follow proper water prep guidelines

385 plant species in Europe are blooming earlier than ever.

In U.S. and Canada, ragweed season is up to **27 days longer.**

Allergic rhinitis generates more than **12 million doctor visits** each year.

35 million Americans are allergic to pollen and mold.

Common spring allergies

- Tree and grass pollen
- Mold spores
- Dust mites & cockroaches
- Animal dander

njhealth.org
1.877.CALL NJH (877.225.5654)

National Jewish Health®
Science Transforming Life®

U.S. DEPARTMENT OF ENERGY | Fossil Energy and Carbon Management

NATIONAL ENERGY TECHNOLOGY LABORATORY

Annual meeting
DE-FE0032005

Reversible Methane Electrochemical Reactor as an Efficient Energy Storage for Fossil Power Generation

Pejman Kazempoor, Ph.D (OU)

Chuancheng Duan, Ph.D. (KSU)

April 20, 2023

Sustainable Energy and Carbon Management Center

Sustainable and Alternative Energy Sources

Carbon Management

Sustainable Energy and Carbon Management Center

For more information, please contact Dr. Pejman Kazempoor (pkazempoor@ou.edu)

Smart Production Through Digitization

Energy Storage and Management

Developing solutions that are locally appropriate; socially beneficial; economically and technically feasible; and environmentally responsible.

AOI 3: Innovative Concepts & Technologies

"Substantial number of energy storage technologies are relatively **early-stage** in their development. …The technologies need additional R&D to clarify their current state, understand their suitability for future advancement and integration, and to advance their maturity through R&D."

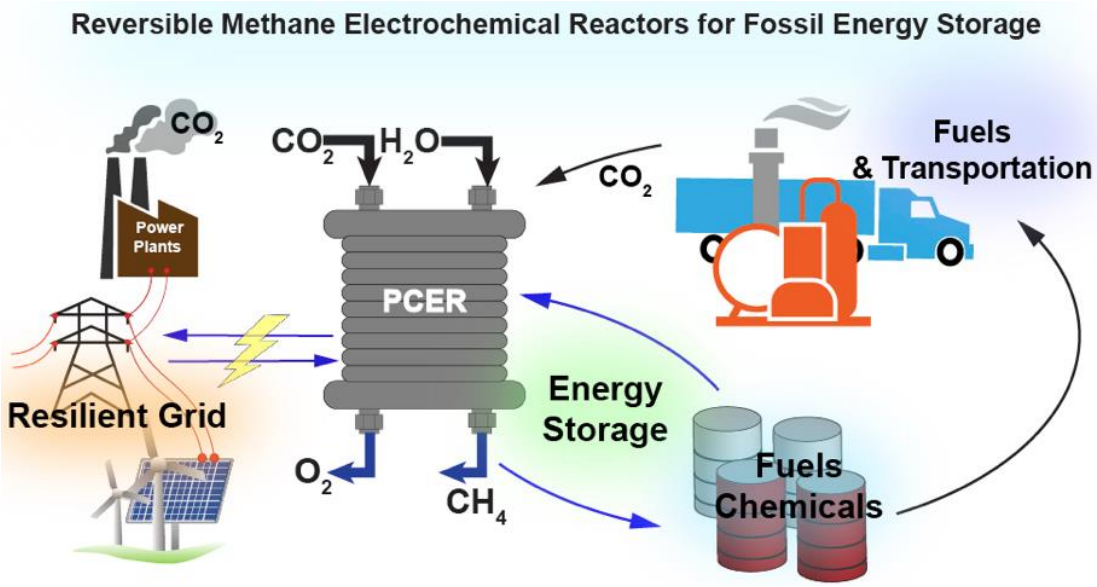

Protonic ceramic electrochemical reactor

Project Objectives

Conduct a comprehensive R&D program to demonstrate the suitability and future advancement and integration of reversible methane electrochemical reactors as an Efficient Energy Storage (EES) with fossil fuel power plants.

Distinguish feature of the proposed technology

1- Direct Integration with fossil assets including fossil power plants and fossil-fuel industrial applications

2- PCERs exhibit high H_2S tolerance and coking tolerance

3- Reversible methane electrochemical cells display a high theoretical round-trip efficiency

4- Reduced operating temperatures enable hybridization with a broader range of waste heat sources

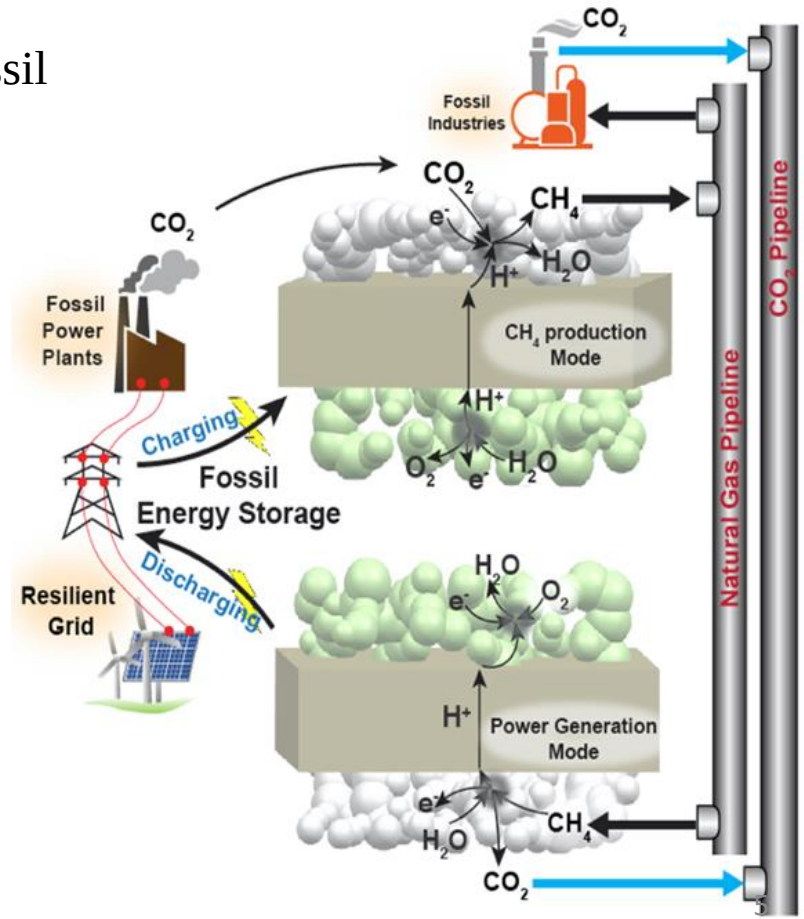

Technology integration with existing or new fossil assets

Indirect integration: CO_2 is captured and separated through an intermediate system before entering the reversible PCER.

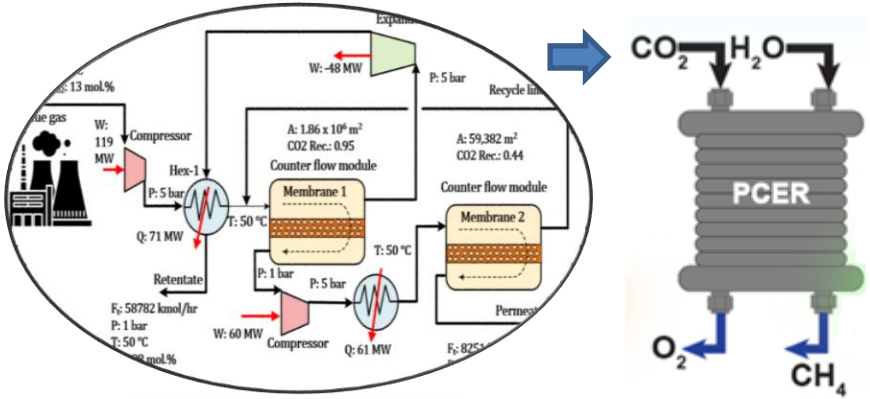

Direct integration: the flue gas enters the system without additional complex separation and purification processes to capture CO_2, allowing significant cost reduction.

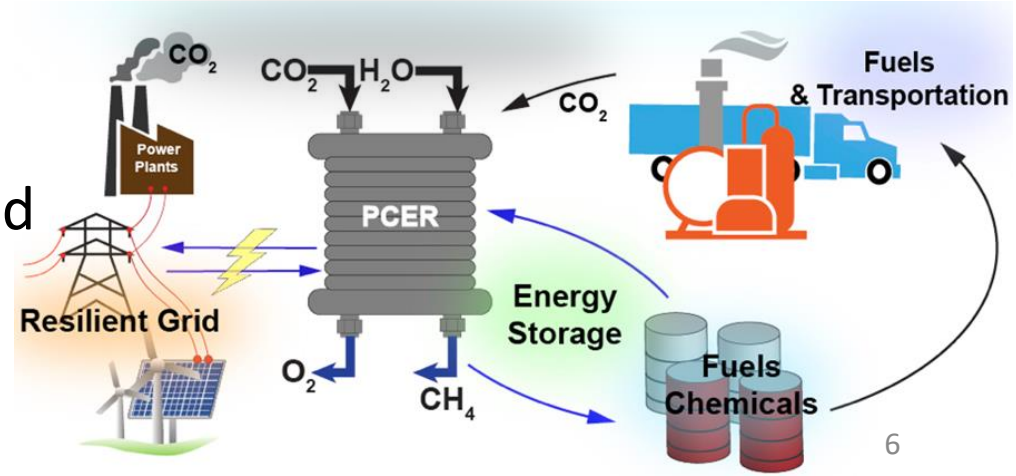

Define the Proposed Energy Storage Technology

Systems Design Processes

1. Characterize the initial state

2. Identify references to accomplish the general objective

3. Specify the proposed energy storage as the desire end states;

4. Define and consolidate the parameters and processes required to transform the initial energy storage technology into the desired end states

5. Assess the respective development or deployment status of the technology required for each function to yield technology needs.

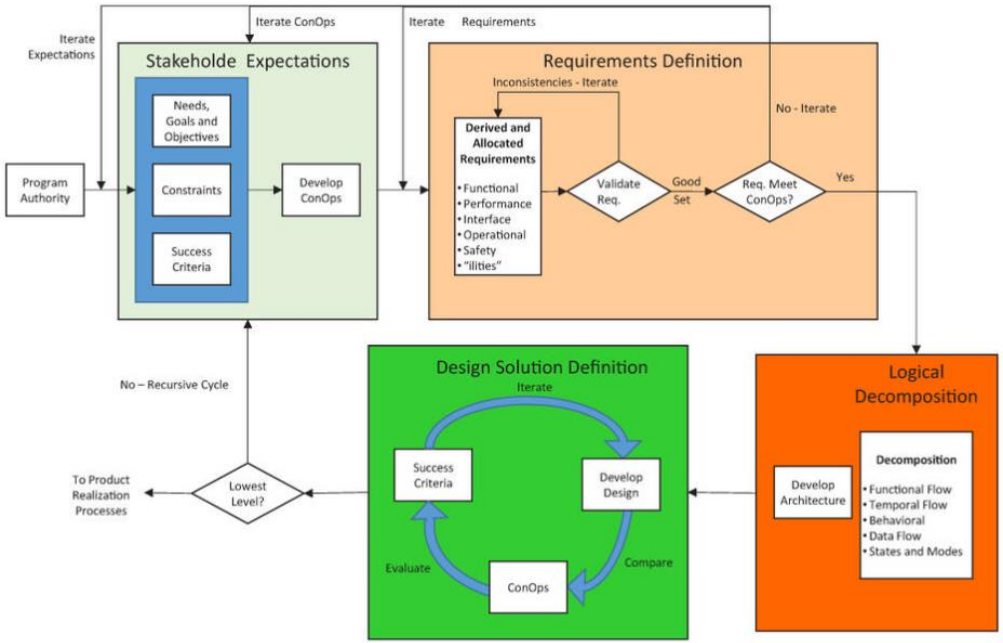

[2] Interrelationships among the System Design Processes. NASA

[1] https://pragmaticarchitect.wordpress.com/2013/05/14/how-to-build-a-roadmap-define-end-state/
[2] https://www.nasa.gov/seh/2-fundamentals

DOE Status and Targets for Reversible Solid Oxide Performance and Cost

- Stack cost target of $225/kW
- System cost target of $900/kW
- Less than 0.2% per 1,000 hours over an operating lifetime of 40,000 hours
- Efficiency of greater than 60% without carbon capture and storage

Metric	2018 Status	2020 Targets	2025/2030 Targets
System Cost ($/kWe)	>12,000	6,000	900
System Degradation (%/1000 hrs)	1-1.5	0.5-1.0	>0.2
Durability (hr)	<2000	5000	8000
Fuel	Natural gas	Natural gas Simulated syngas	Natural gas Coal-derived syngas
Demonstration Scale	50 kWe – 200 kWe	200 kWe – 1 MWe	10-50 MWe

Recent development of cell configuration to increase current density

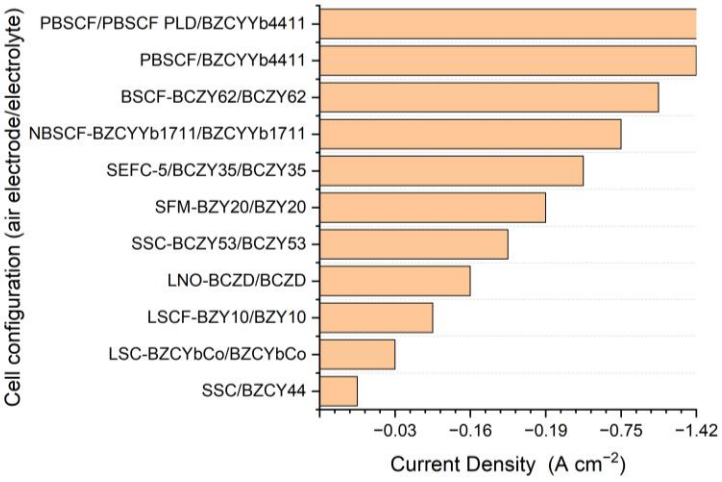

Compositions of electrolyte (E) and cathode (C)*	Power density	Features	Year	Refs
E: $BaCe_{0.7}Zr_{0.1}Y_{0.2}O_{3-\delta}$ (10 μm) C: $La_{0.5}Sr_{0.5}Fe_{0.9}Mo_{0.1}O_{3-\delta}$	650 °C: 851 mW cm^{-2} 700 °C: 1174 mW cm^{-2}	Modification of $La_{0.5}Sr_{0.5}FeO_{3-\delta}$ with molybdenum	2021	31
E: $BaCe_{0.7}Zr_{0.1}Y_{0.2}O_{3-\delta}$ (15 μm) C: $La_{0.5}Ca_{0.5}MnO_{3-\delta}$	600 °C: 486 mW cm^{-2} 650 °C: 701 mW cm^{-2} 700 °C: 1155 mW cm^{-2}	Modification of $LaMnO_3$ with calcium	2021	32
E: $BaCe_{0.7}Zr_{0.1}Y_{0.1}Yb_{0.1}O_{3-\delta}$ (25 μm) C: $Ba(Co_{0.4}Fe_{0.4}Zr_{0.1}Y_{0.1})_{0.95}Ni_{0.05}O_{3-\delta}$	500 °C: 270 mW cm^{-2} 550 °C: 450 mW cm^{-2} 600 °C: 660 mW cm^{-2}	Development of a new triple-conducting electrode with improved electrochemical activity and reduced thermal expansion	2021	33
E: $BaCe_{0.7}Zr_{0.1}Y_{0.1}Yb_{0.1}O_{3-\delta}$ (24 μm) C: $La_{0.5}(Ba_{0.75}Ca_{0.25})_{0.5}Co_{0.8}Fe_{0.2}O_{3-\delta}$	600 °C: 311 mW cm^{-2} 650 °C: 489 mW cm^{-2} 700 °C: 716 mW cm^{-2}	Ca-doping of $La_{0.5}Ba_{05}Co_{0.8}Fe_{0.2}O_{3-\delta}$ improves electrocatalytical activity and reduces thermal expansion	2021	34
E: $BaCe_{0.7}Zr_{0.1}Y_{0.1}Yb_{0.1}O_{3-\delta}$ (30 μm) C: $La_{0.25}Sr_{2.75}FeNiO_{7-\delta}$–$BaCe_{0.7}Zr_{0.1}Y_{0.1}Yb_{0.1}O_{3-\delta}$	500 °C: 95 mW cm^{-2} 550 °C: 187 mW cm^{-2} 600 °C: 334 mW cm^{-2}	Development of a new Ruddlesden-Popper electrode	2021	35
E: $BaCe_{0.7}Zr_{0.1}Y_{0.1}Yb_{0.1}O_{3-\delta}$ (14 μm) C: $La_{0.6}Sr_{0.4}Co_{0.2}Fe_{0.8}O_{3-\delta}$–$BaCe_{0.7}Zr_{0.1}Y_{0.1}Yb_{0.1}O_{3-\delta}$	500 °C: 240 mW cm^{-2} 550 °C: 380 mW cm^{-2} 600 °C: 570 mW cm^{-2}	Introduction of a porous $BaCe_{0.7}Zr_{0.1}Y_{0.1}Yb_{0.1}O_{3-\delta}$ interlayer between E and C	2021	36
E: $BaCe_{0.7}Zr_{0.1}Y_{0.1}Yb_{0.1}O_{3-\delta}$ (25 μm) C: $La_{0.6}Sr_{0.4}Co_{0.2}Fe_{0.8}O_{3-\delta}$–$BaCe_{0.7}Zr_{0.1}Y_{0.1}Yb_{0.1}O_{3-\delta}$	500 °C: 188 mW cm^{-2} 550 °C: 294 mW cm^{-2} 600 °C: 465 mW cm^{-2}	Tubular PCFC with a working electrode area of 2.3 cm^2	2021	37
E: $BaCe_{0.6}Zr_{0.2}Y_{0.1}Yb_{0.1}O_{3-\delta}$ (11 μm) C: $PrBa_{0.5}Sr_{0.5}Co_{1.5}Fe_{0.5}O_{5+\delta}$	500 °C: 420 mW cm^{-2} 550 °C: 625 mW cm^{-2} 600 °C: 815 mW cm^{-2}	A Pd interlayer is introduced between E and C to improve the interface electrochemical reactions	2021	38
E: $BaCe_{0.7}Zr_{0.1}Y_{0.2}O_{3-\delta}$ (42 μm) C: $BaCe_{0.2}Fe_{0.6}Pr_{0.2}O_{3-\delta}$	600 °C: 316 mW cm^{-2} 650 °C: 447 mW cm^{-2} 700 °C: 562 mW cm^{-2}	Pr-doping of a $BaCe_{0.2}Fe_{0.8}O_3$ electrode is performed to enhance its electrochemical activity	2021	39
E: $BaCe_{0.7}Zr_{0.1}Y_{0.2}O_{3-\delta}$ (15 μm) C: $BaFe_{0.8}Ce_{0.1}Y_{0.1}O_{3-\delta}$	550 °C: 237 mW cm^{-2} 600 °C: 417 mW cm^{-2} 650 °C: 530 mW cm^{-2}	A new triple-conducting electrode of $BaFe_{0.8}Ce_{0.1}Y_{0.1}O_{3-\delta}$ is proposed	2021	40
E: $BaCe_{0.6}Zr_{0.2}Y_{0.1}Yb_{0.1}O_{3-\delta}$ (15.7 μm) C: $PrBa_{0.5}Sr_{0.5}Co_{1.5}Fe_{0.5}O_{5+\delta}$	500 °C: 414 mW cm^{-2} 600 °C: 685 mW cm^{-2} 700 °C: 950 mW cm^{-2}	This work confirms excellent electrochemical behavior of a $PrBa_{0.5}Sr_{0.5}Co_{1.5}Fe_{0.5}O_{5+\delta}$ triple-conducting material	2021	41
E: $BaCe_{0.7}Zr_{0.1}Y_{0.2}O_{3-\delta}$ (15 μm) C: $Sr_2Fe_{1.5}Mo_{0.25}Sc_{0.25}O_{6-\delta}$	600 °C: 545 mW cm^{-2} 650 °C: 965 mW cm^{-2} 700 °C: 1254 mW cm^{-2}	This work proposes new oxygen electrode with high electrochemical activity and stability towards CO_2	2022	42
E: $BaCe_{0.7}Zr_{0.1}Y_{0.2}O_{3-\delta}$ (8 μm) C: $LaNi_{0.6}Fe_{0.4}O_{3-\delta}$–$Sm_{0.5}Sr_{0.5}CoO_{3-\delta}$	600 °C: 425 mW cm^{-2} 650 °C: 728 mW cm^{-2} 700 °C: 1427 mW cm^{-2}	A new combination of perovskite and layered structured materials is proposed to be used as a cathode for PCFCs	2022	43
E: $BaCe_{0.6}Zr_{0.2}Y_{0.1}Yb_{0.1}O_{3-\delta}$ (15 μm) C: $Ba_{0.95}(Co_{0.4}Fe_{0.4}Zr_{0.1}Y_{0.1})_{0.95}Ni_{0.05}O_{3-\delta}$	500 °C: 262 mW cm^{-2} 550 °C: 450 mW cm^{-2} 600 °C: 672 mW cm^{-2}	A complex modification (Ba-deficiency and Ni-doping) has been proposed for improving functional properties of the-state-of-the-art triple-conducting $BaCo_{0.4}Fe_{0.4}Zr_{0.1}Y_{0.1}O_{3-\delta}$ material	2022	44
E: $BaCe_{0.6}Zr_{0.2}Y_{0.1}Yb_{0.1}O_{3-\delta}$ (15.7 μm) C: $SrCo_{0.4}Fe_{0.4}Zr_{0.1}Y_{0.1}O_{3-\delta}$–$BaCe_{0.6}Zr_{0.2}Y_{0.1}Yb_{0.1}O_{3-\delta}$	500 °C: 171 mW cm^{-2} 550 °C: 278 mW cm^{-2} 600 °C: 409 mW cm^{-2}	This work reports a successful application of $SrCo_{0.4}Fe_{0.4}Zr_{0.1}Y_{0.1}O_{3-\delta}$-based electrodes	2022	45

* Anode materials are not detailized in their compositions, since they (in oxidized forms) consist of NiO mixed with the electrolyte (E).

Kobayashi, T., Kuroda, K., Jeong, S., Kwon, H., Zhu, C., Habazaki, H., & Aoki, Y. (2018). Analysis of the anode reaction of solid oxide electrolyzer cells with BaZr0. 4Ce0. 4Y0. 2O3-δ electrolytes and Sm0. 5Sr0. 5CoO3-δ anodes. Journal of The Electrochemical Society, 165(5), F342.

Choi, S., Davenport, T. C., & Haile, S. M. (2019). Protonic ceramic electrochemical cells for hydrogen production and electricity generation: exceptional reversibility, stability, and demonstrated faradaic efficiency. Energy & Environmental Science, 12(1), 206-215.

Huan, D., Shi, N., Zhang, L., Tan, W., Xie, Y., Wang, W., ... & Lu, Y. (2018). New, efficient, and reliable air electrode material for proton-conducting reversible solid oxide cells. ACS applied materials & interfaces, 10(2), 1761-1770.

Kim, J., Jun, A., Gwon, O., Yoo, S., Liu, M., Shin, J., ... & Kim, G. (2018). Hybrid-solid oxide electrolysis cell: A new strategy for efficient hydrogen production. Nano Energy, 44, 121-126.

Cost Benchmarking of PCFC Versus SOFCs: (a) Cell and Balance-Of-Stack Component and (b) Total Stack Cost Distributions.

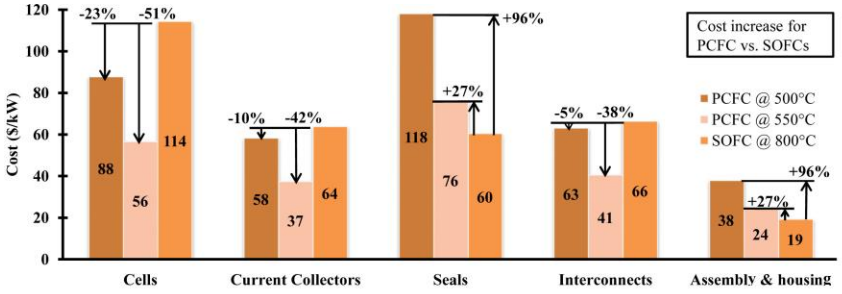

(a)

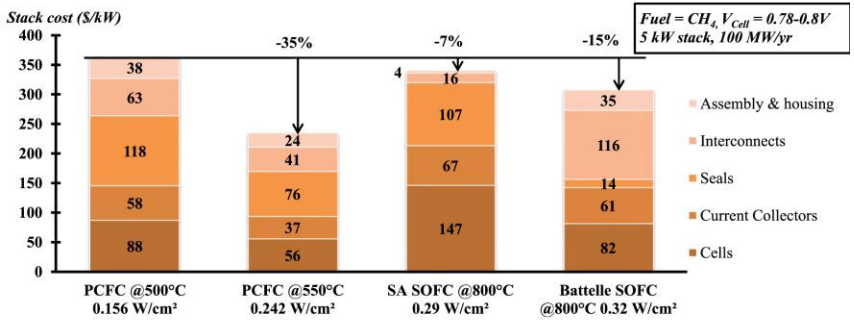

(b)

$$C_{cell} = \sum_{processes} (C_{mat} + C_{elec} + C_{labor} + C_{mach})$$

$$C_{mat}\left[\$\ kWh^{-1}\right] = \frac{m_{cell}\ [kg\ cell^{-1}] * p_{mat}\ [\$\ kg^{-1}]}{A_{cell}\ [cm^2\ cell^{-1}] * p_{cell}\ [kW\ cm^{-2}]}$$

A significant power density improvement in PCFC or a lower-cost sealant solution for the intermediate operation temperatures of PCFC are required in the future to close the gap of sealant cost with SOFC.

Dubois, A., Ricote, S., & Braun, R. J. (2017). Benchmarking the expected stack manufacturing cost of next generation, intermediate-temperature protonic ceramic fuel cells with solid oxide fuel cell technology. Journal of Power Sources, 369, 65-77.

Technical Targets (by DOE) and Achievements for High-Temperature Reversible Fuel Cells (Cell/Stack level)

SOFC RFC Technical Targets

Characteristic	Units	2020 Status	2030 Targets	Ultimate Targets
Cell Performance/ Roundtrip Electrical Efficiency at 0.5 A/cm2 FC; 1 A/cm² EL	%	80	80	85
Cell Durability/Degradation Rate	%/1000 hr	<1.5	0.25	0.125
Stack Capital Cost (based on FC power output)	$/kW	500	330	300
System				
System Roundtrip Efficiency	%	-	40	50
Roundtrip System Efficiency (includes thermal energy input)	%	37	60	70
Lifetime/Durability	hr [Cycles]	10,000[7] [unknown]	40,000 [1667]	80,000 [3333]
Levelized Cost of Storage	$/kWh	1.11	0.20	0.10[11]
System Capital Cost by Power	$/kW	-	$1750	$1250
System Capital Cost by Energy	$/kWh	-	250	150

https://www.hydrogen.energy.gov/pdfs/review20/fc332_wei_2020_o.pdf

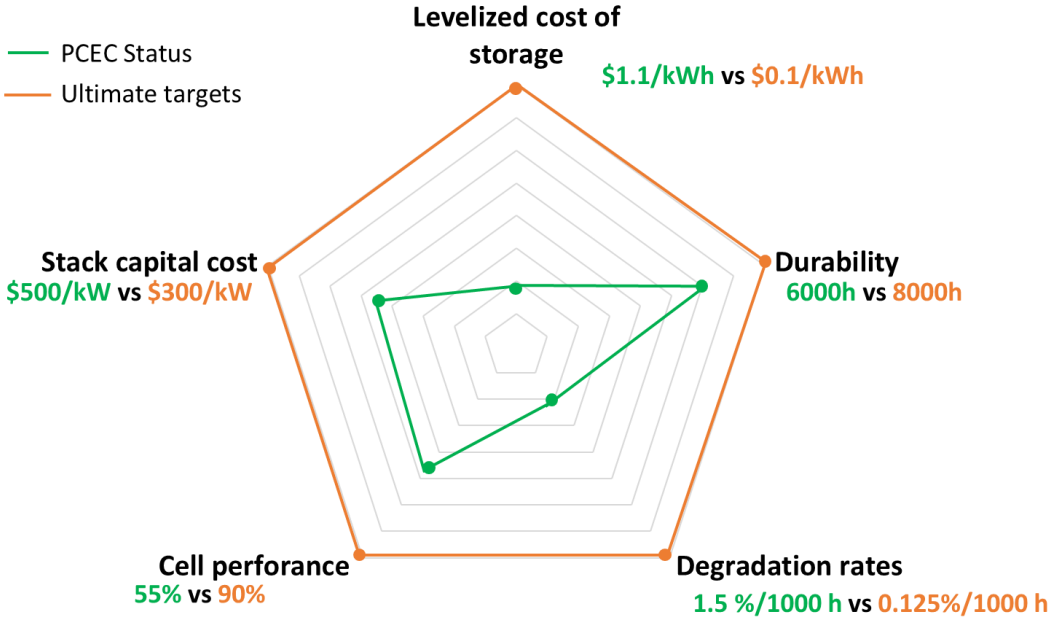

Peterson, D. (2020), Reversible Fuel Cell Targets, DOE Hydrogen and Fuel Cells Program Record : 20001.

Choi, S., Davenport, T. C., & Haile, S. M. (2019). Protonic ceramic electrochemical cells for hydrogen production and electricity generation: exceptional reversibility, stability, and demonstrated faradaic efficiency. Energy & Environmental Science, 12(1), 206-215

Duan, C., Kee, R. J., Zhu, H., Karakaya, C., Chen, Y., Ricote, S., ... & O'Hayre, R. (2018). Highly durable, coking and sulfur tolerant, fuel-flexible protonic ceramic fuel cells. Nature, 557(7704), 217-222.

Experimental Studies to Define Reversible Methane PCER Performance Parameters

Previous Protonic ceramic electrochemical reactor for power generation and chemicals production

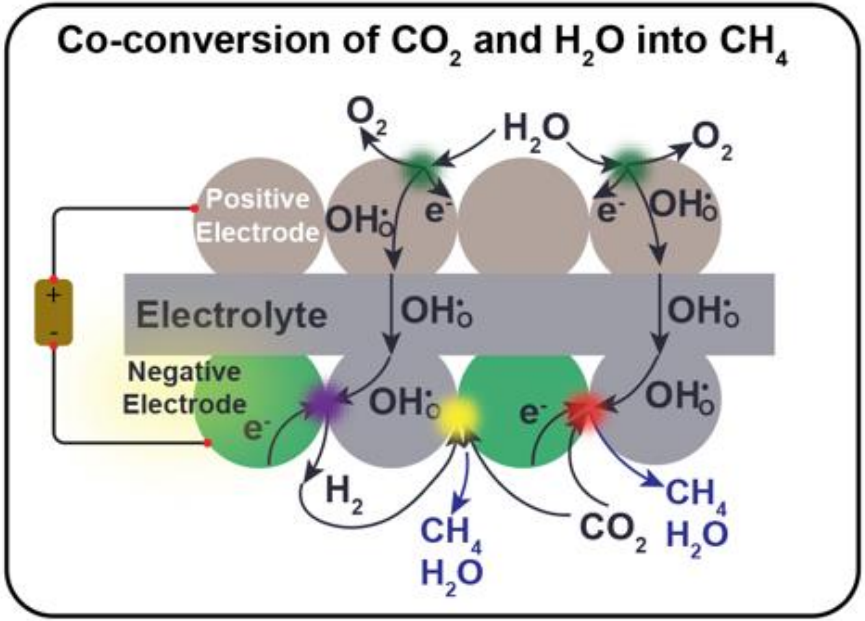

ELSEVIER

Nano Energy

Volume 102, November 2022, 107722

Full paper

Rationally designed negative electrode for selective CO_2-to-CO conversion in protonic ceramic electrochemical cells

Fan Liu [a], Liyang Fang [a], David Diercks [b], Pejman Kazempoor [c], Chuancheng Duan [a]

Show more

+ Add to Mendeley Share Cite

https://doi.org/10.1016/j.nanoen.2022.107722 Get rights and content

Abstract

Protonic ceramic electrochemical cells (PCECs) are solid-state electrochemical devices that employ proton-conducting oxides as electrolytes, which offer a promising approach for electrification of chemical manufacturing, including CO_2 reduction to produce value-added chemicals (e.g., CO). The primary advantage of PCECs is their intermediate operating temperatures (300–600°C), which thermodynamically and kinetically favor the CO_2 reduction chemistry at the negative electrode. However, the conventional negative electrodes of PCECs, such as $BaZr_{0.8-x}Ce_xY_{0.2}O_{3-\delta}$-Ni or $BaZr_{0.8-x}Ce_xY_{0.1}Yb_{0.1}O_{3-\delta}$-Ni, cannot reduce CO_2 to either CH_4 or CO with a selectivity of >99 %, leading to the

Research Activity 1 at KSU: high-performance protonic ceramic fuel cells (PCFCs)

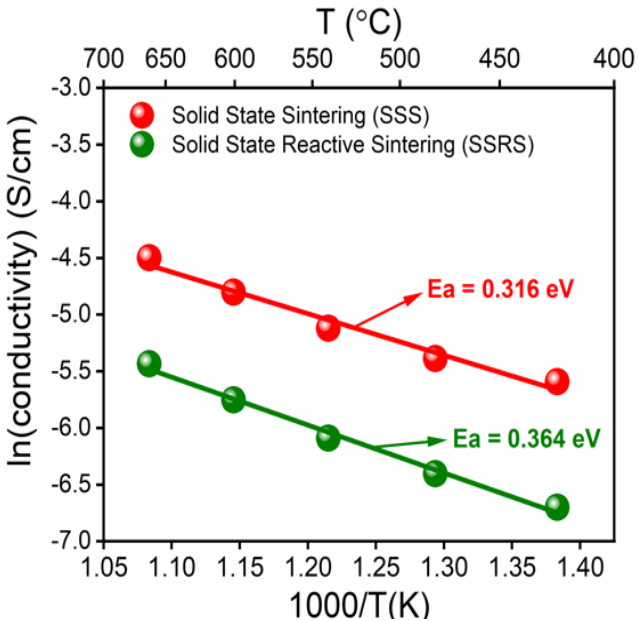

Figure 1. $BaCe_{0.4}Zr_{0.4}Y_{0.1}Yb_{0.1}O_3$ electrolyte membrane conductivity of PCECs fabricated via SSS and SSRS.

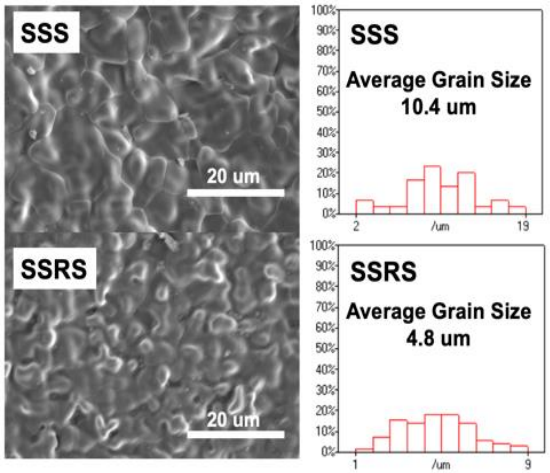

Figure 2. SEM images and grain size of electrolyte membrane of PCECs fabricated via SSS and SSRS.

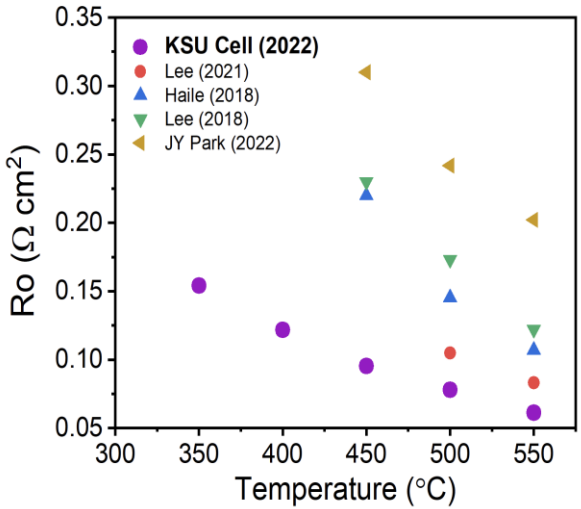

Figure 3. The Ultra-high-performance PCFC demonstrated at KSU exhibits the lowest Ohmic resistance.

Highly conductive electrolyte membrane

Research Activity 1 at KSU: high-performance protonic ceramic fuel cells (PCFCs)

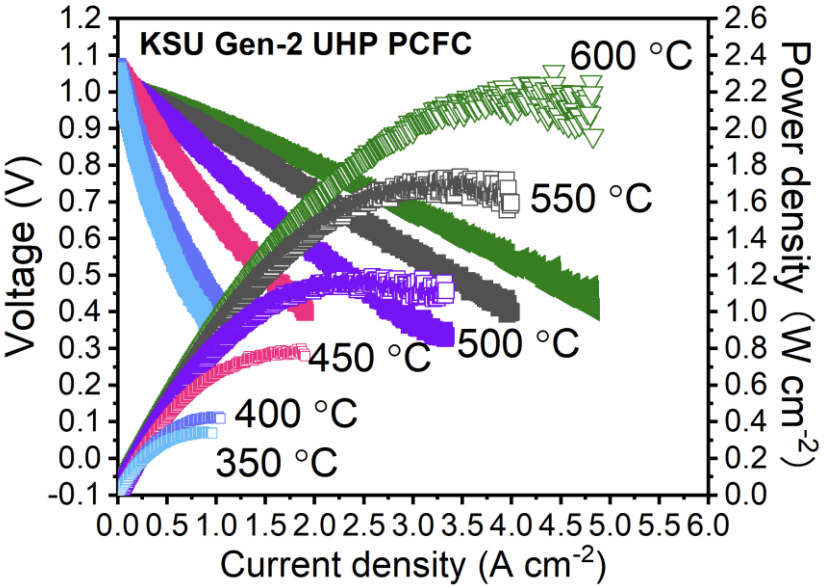

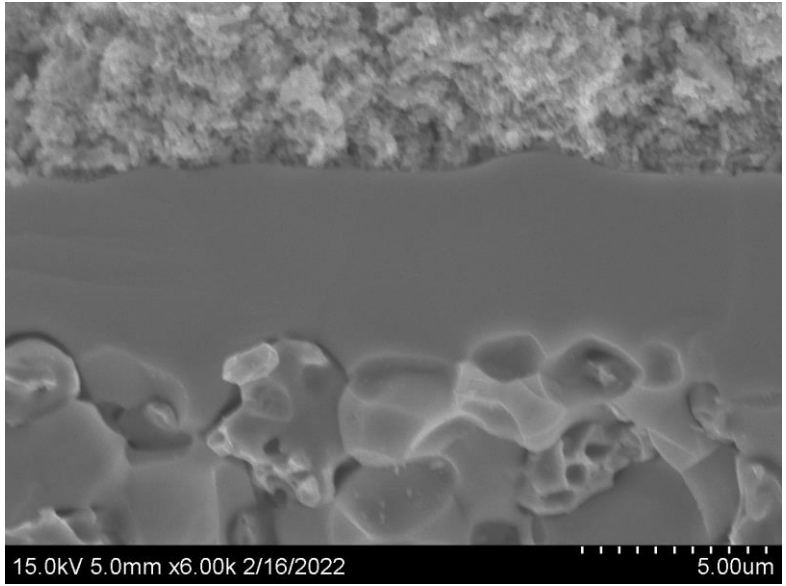

Figure 1. Ultra-high-performance KSU Gen-2 PCFC recently demonstrated at KSU.

Word record PCFC performances

Research Activity 1 at KSU: high-performance protonic ceramic fuel cells

First SEM single anode layer

~0.35 W/cm²@600°C

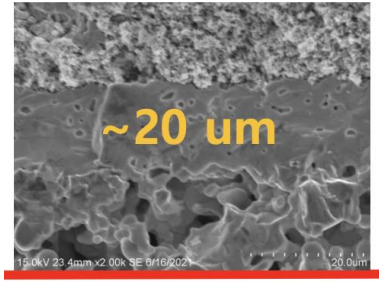

Double SSR anode layer

~0.9 W/cm² @600°C
Very unstable
Difficult to reproduce

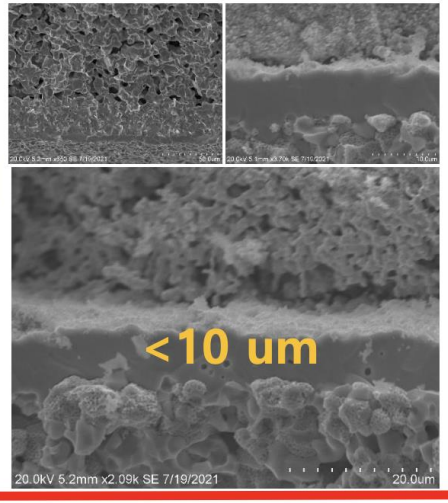

Double SSR anode layer

Electrolyte ink optim.
~0.5 W/cm² @600°C
Very unstable

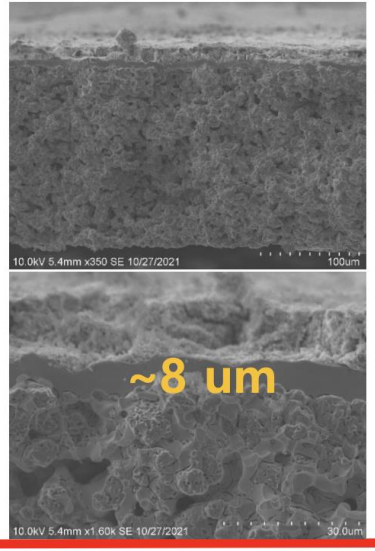

Double SSS anode

Good stability

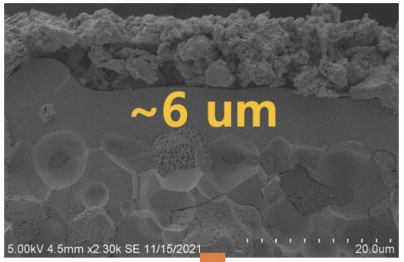

Optimization

~1.8 W/cm² @600°C
Good stability

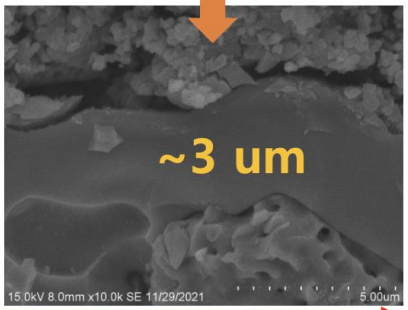

June → **July-Aug** → **Sep-Oct** → **Nov-Dec**

Research Activity 1 at KSU: high-performance protonic ceramic fuel cells (PCFCs)

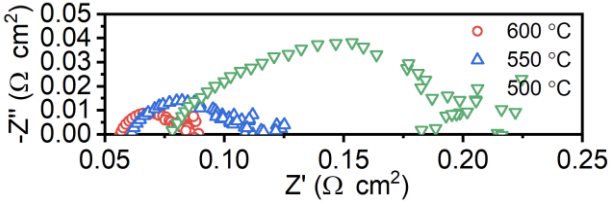

Figure 1. EIS spectra of KSU Gen-2 PCFC at 500-600 ºC.

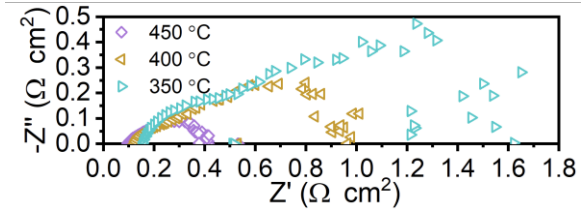

Figure 2. EIS spectra of KSU Gen-2 PCFC at 350-450 ºC.

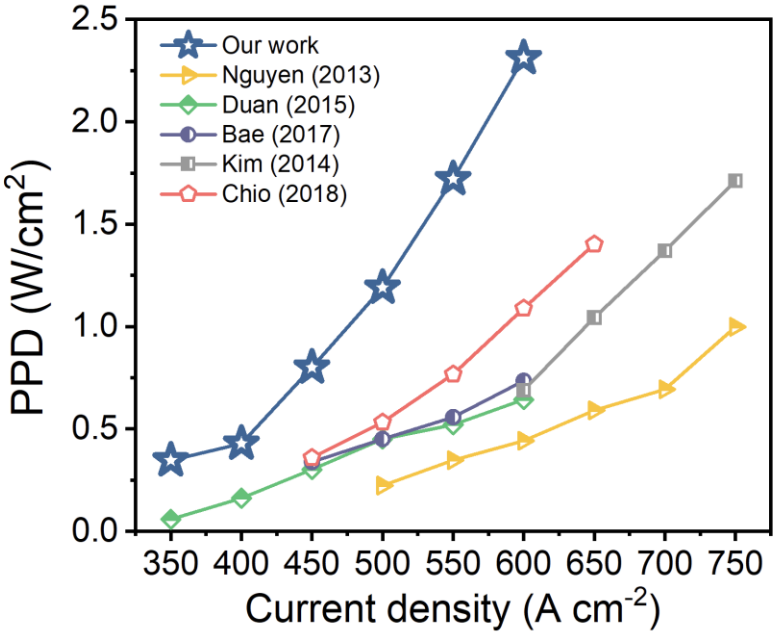

Highly active electrodes at intermediate operating temperatures

Reduced operating temperature favors CO_2 methanation

Research Activity 1 at KSU: high-performance protonic ceramic fuel cells (PCFCs)

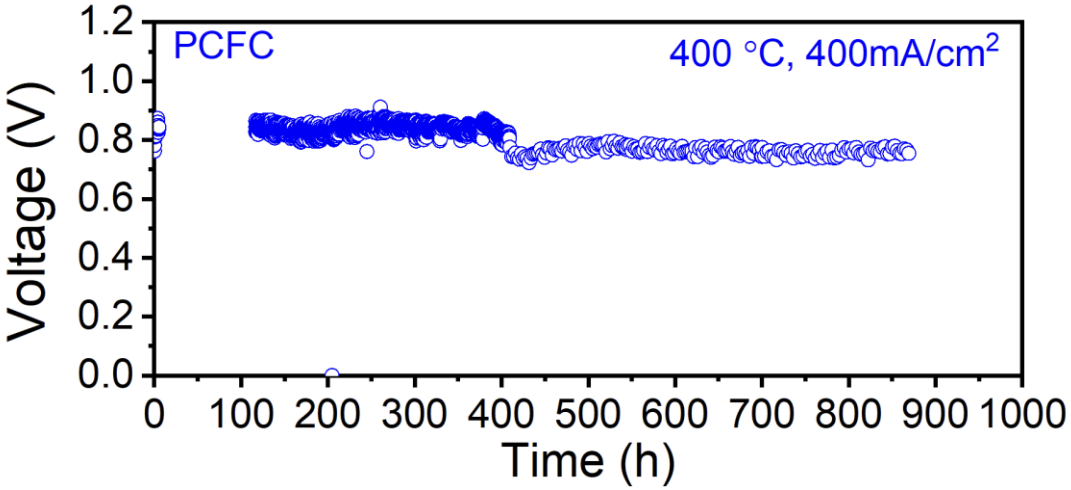

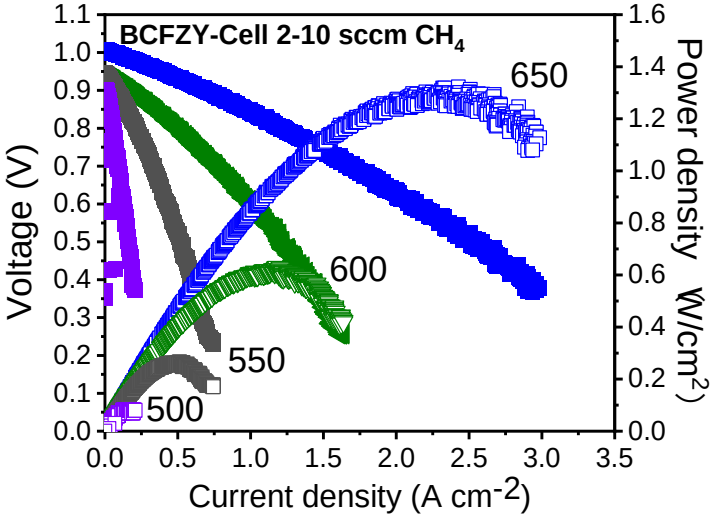

Durable PCFC performances at intermediate operating temperatures

Word record PCFC performances under methane

Research Activity 2 at KSU: CO_2 methanation catalysts

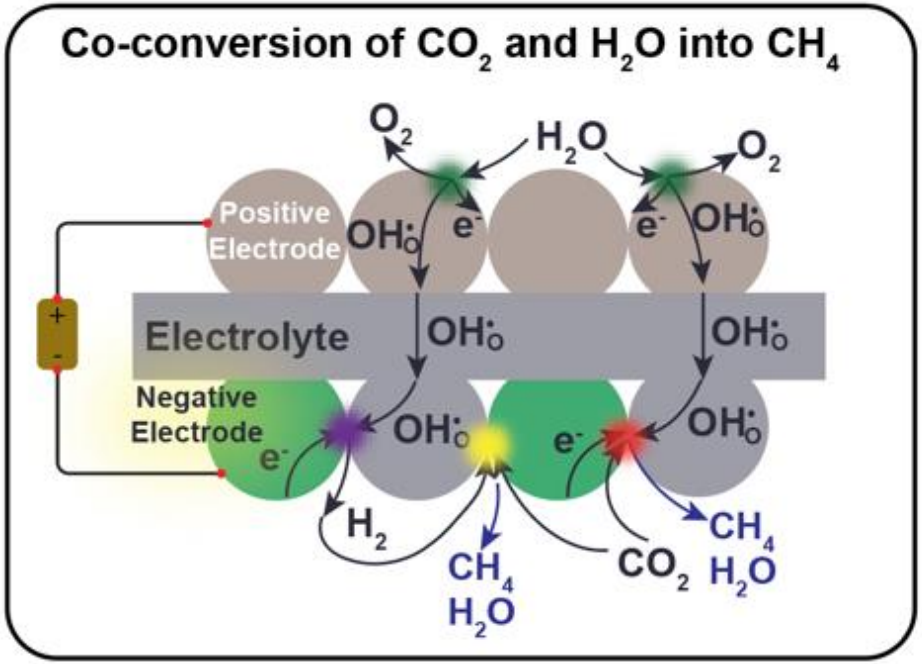

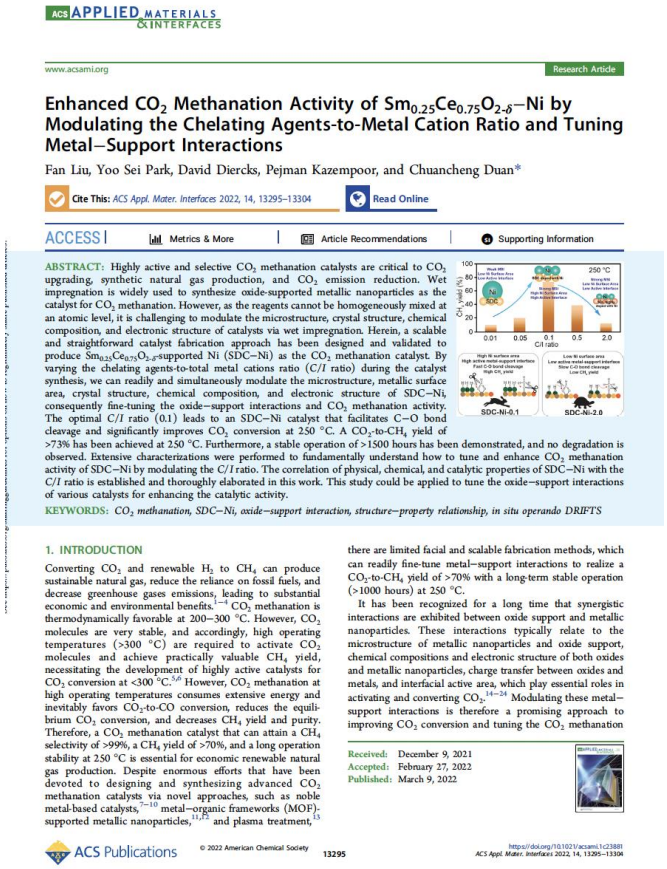

ACS APPLIED MATERIALS & INTERFACES

www.acsami.org Research Article

Enhanced CO_2 Methanation Activity of $Sm_{0.25}Ce_{0.75}O_{2-\delta}$–Ni by Modulating the Chelating Agents-to-Metal Cation Ratio and Tuning Metal–Support Interactions

Fan Liu, Yoo Sei Park, David Diercks, Pejman Kazempoor, and Chuancheng Duan*

Cite This: *ACS Appl. Mater. Interfaces* 2022, 14, 13295−13304 Read Online

ACCESS | Metrics & More | Article Recommendations | Supporting Information

ABSTRACT: Highly active and selective CO_2 methanation catalysts are critical to CO_2 upgrading, synthetic natural gas production, and CO_2 emission reduction. Wet impregnation is widely used to synthesize oxide-supported metallic nanoparticles as the catalyst for CO_2 methanation. However, as the reagents cannot be homogeneously mixed at an atomic level, it is challenging to modulate the microstructure, crystal structure, chemical composition, and electronic structure of catalysts via wet impregnation. Herein, a scalable and straightforward catalyst fabrication approach has been designed and validated to produce $Sm_{0.25}Ce_{0.75}O_{2-\delta}$-supported Ni (SDC−Ni) as the CO_2 methanation catalyst. By varying the chelating agents-to-total metal cations ratio (C/I ratio) during the catalyst synthesis, we can readily and simultaneously modulate the microstructure, metallic surface area, crystal structure, chemical composition, and electronic structure of SDC−Ni, consequently fine-tuning the oxide−support interactions and CO_2 methanation activity. The optimal C/I ratio (0.1) leads to an SDC−Ni catalyst that facilitates C−O bond cleavage and significantly improves CO_2 conversion at 250 °C. A CO_2-to-CH_4 yield of >73% has been achieved at 250 °C. Furthermore, a stable operation of >1500 hours has been demonstrated, and no degradation is observed. Extensive characterizations were performed to fundamentally understand how to tune and enhance CO_2 methanation activity of SDC−Ni by modulating the C/I ratio. The correlation of physical, chemical, and catalytic properties of SDC−Ni with the C/I ratio is established and thoroughly elaborated in this work. This study could be applied to tune the oxide−support interactions of various catalysts for enhancing the catalytic activity.

KEYWORDS: *CO_2 methanation, SDC−Ni, oxide−support interaction, structure−property relationship, in situ operando DRIFTS*

1. INTRODUCTION

Converting CO_2 and renewable H_2 to CH_4 can produce sustainable natural gas, reduce the reliance on fossil fuels, and decrease greenhouse gases emissions, leading to substantial economic and environmental benefits.[1−4] CO_2 methanation is thermodynamically favorable at 200−300 °C. However, CO_2 molecules are very stable, and accordingly, high operating temperatures (>300 °C) are required to activate CO_2 molecules and achieve practically valuable CH_4 yield, necessitating the development of highly active catalysts for CO_2 conversion at <300 °C.[5,6] However, CO_2 methanation at high operating temperatures consumes extensive energy and inevitably favors CO_2-to-CO conversion, reduces the equilibrium CO_2 conversion, and decreases CH_4 yield and purity. Therefore, a CO_2 methanation catalyst that can attain a CH_4 selectivity of >99%, a CH_4 yield of >70%, and a long operation stability at 250 °C is essential for economic renewable natural gas production. Despite enormous efforts that have been devoted to designing and synthesizing advanced CO_2 methanation catalysts via novel approaches, such as noble metal-based catalysts,[7−10] metal−organic frameworks (MOF)-supported metallic nanoparticles,[11,12] and plasma treatment,[13] there are limited facial and scalable fabrication methods, which can readily fine-tune metal−support interactions to realize a CO_2-to-CH_4 yield of >70% with a long-term stable operation (>1000 hours) at 250 °C.

It has been recognized for a long time that synergistic interactions are exhibited between oxide support and metallic nanoparticles. These interactions typically relate to the microstructure of metallic nanoparticles and oxide support, chemical compositions and electronic structure of both oxides and metallic nanoparticles, charge transfer between oxides and metals, and interfacial active area, which play essential roles in activating and converting CO_2.[14−24] Modulating these metal−support interactions is therefore a promising approach to improving CO_2 conversion and tuning the CO_2 methanation

Received: December 9, 2021
Accepted: February 27, 2022
Published: March 9, 2022

https://doi.org/10.1021/acsami.1c23881
ACS Appl. Mater. Interfaces 2022, 14, 13295−13304

Research Activity 2 at KSU: CO_2 methanation catalysts

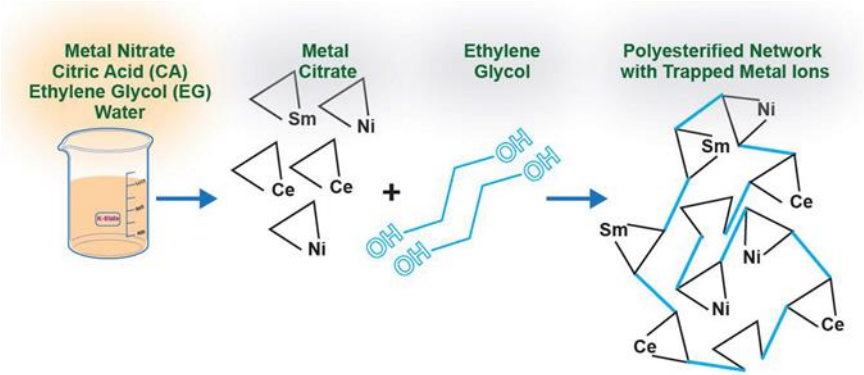

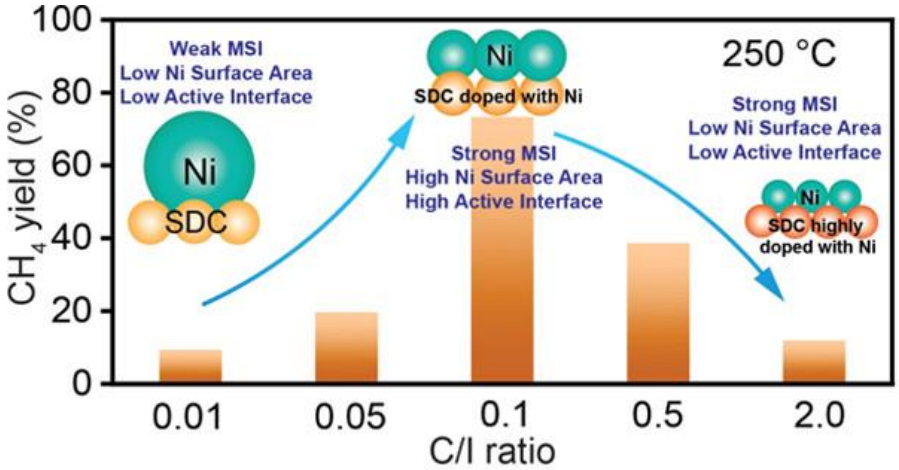

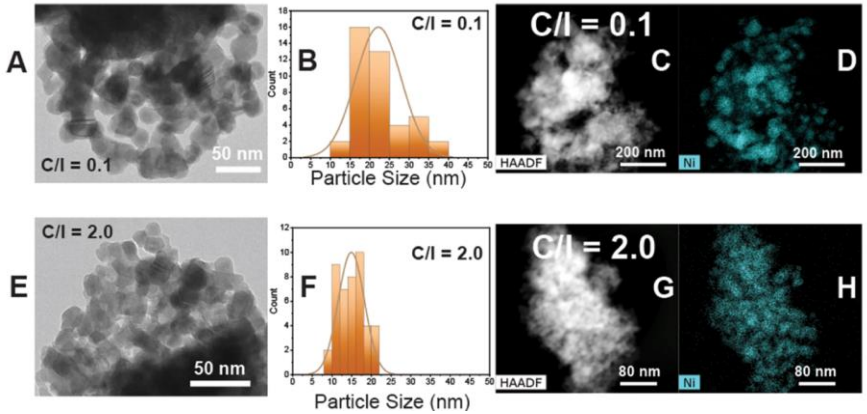

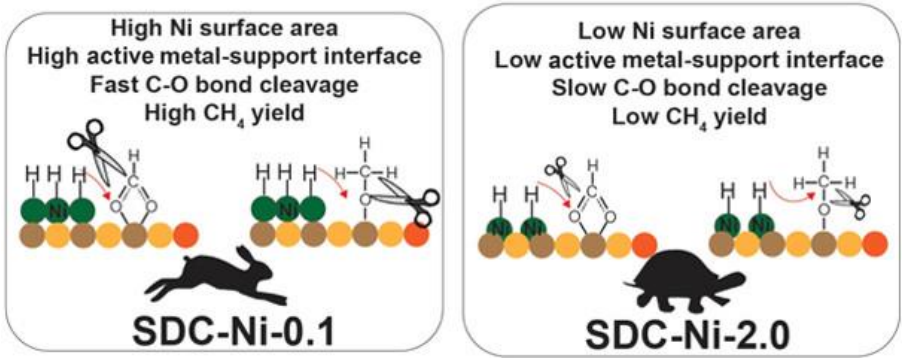

CO_2 methanation catalyst synthesis approach by adjusting **chelating agent/ion ratios (C/I)**

Research Activity 3 at KSU: CO_2 conversion in PCECs

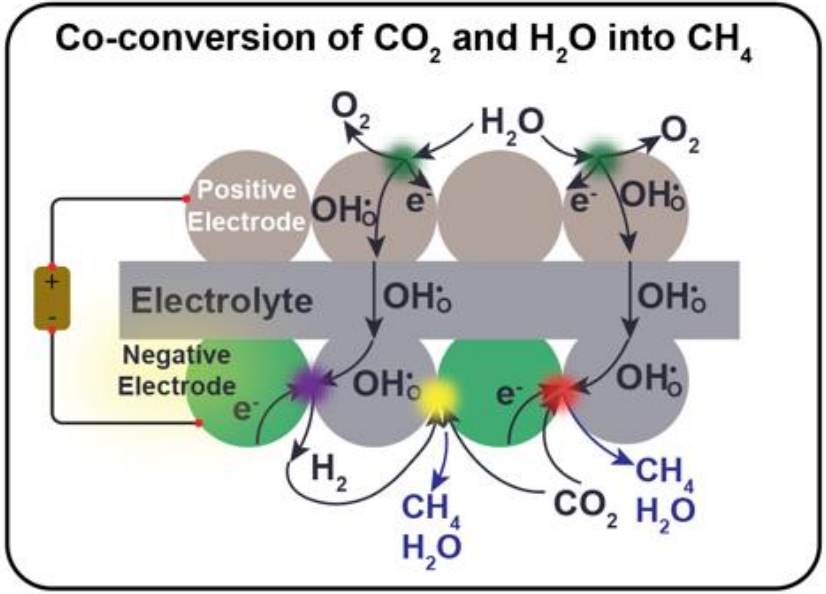

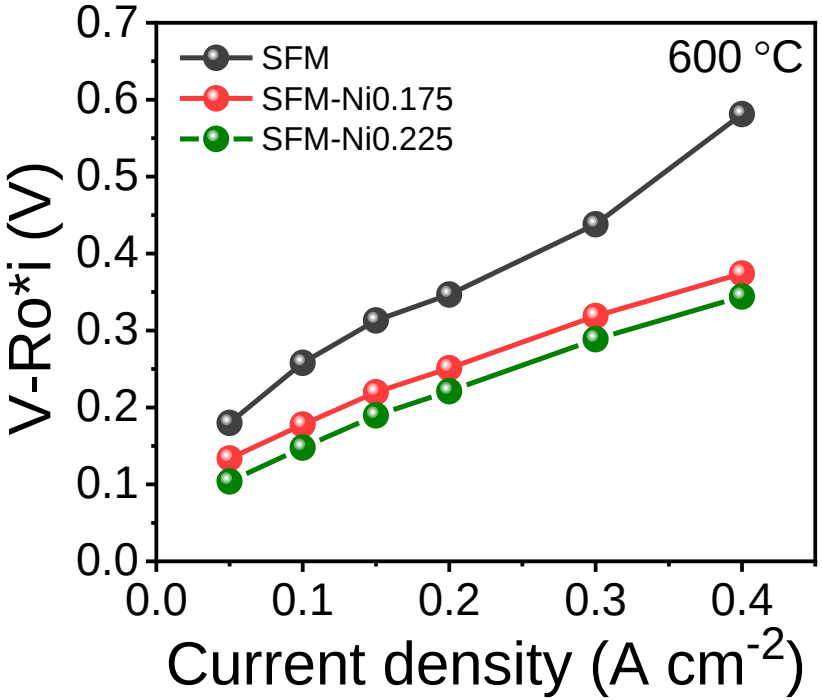

OU-Comprehensive Computational Modeling of Reversible Methane PCER

$$CO + 3H_2 = CH_4 + H_2O \ (\Delta H_{298} = -206 \text{ kJ mol}^{-1}),$$

$$CO_2 + 4H_2 = CH_4 + 2H_2O \ (\Delta H_{298} = -165 \text{ kJ mol}^{-1}),$$

Methane is formed through CO/CO2 hydrogenation.

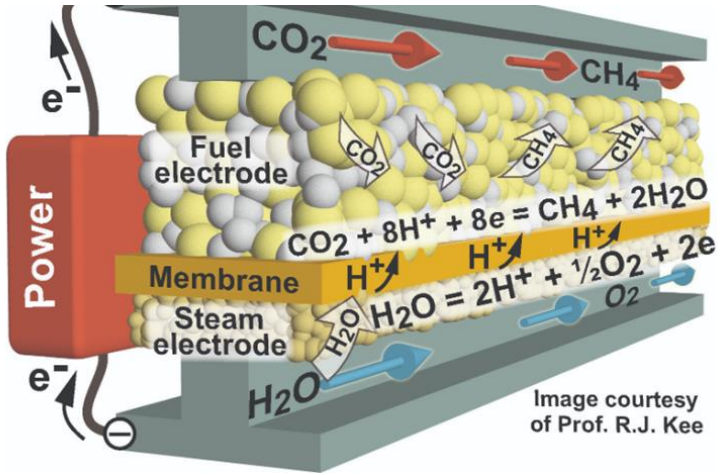

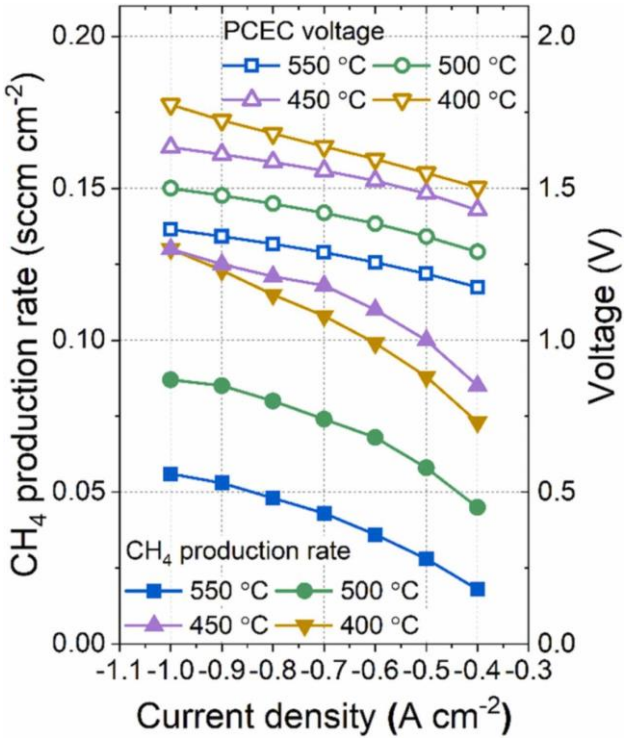

Composite electrodes must deliver multiple physical processes: Gas, ion, and electron transport; catalysis; and electrochemistry

Cell performance depends on the chemical potential of fuel and oxidizer and on internal losses

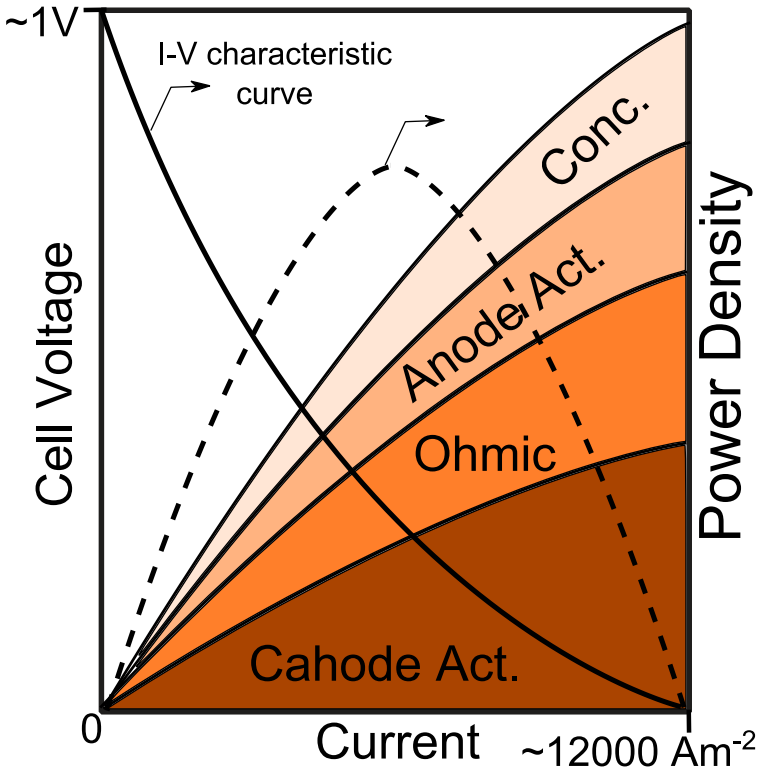

- Nernst potential equation based on the active species in each channel
- Cell operating voltage

$$E_{op,f} = \delta * E_{op,i}$$
$$= \delta * [E_{Nernst,tot} - (\eta_{ohm} + \eta_{act} + \eta_{conc})]$$

η_{ohm}, η_{act} and η_{conc} are the ohmic, activation and concentration overpotentials

- Adjustment factor, δ

$$\delta = 0.00218 * T_{PEN} - 1.0683$$

T_{PEN} is the cell operating temperature in Kelvin

Model validation at different temperatures

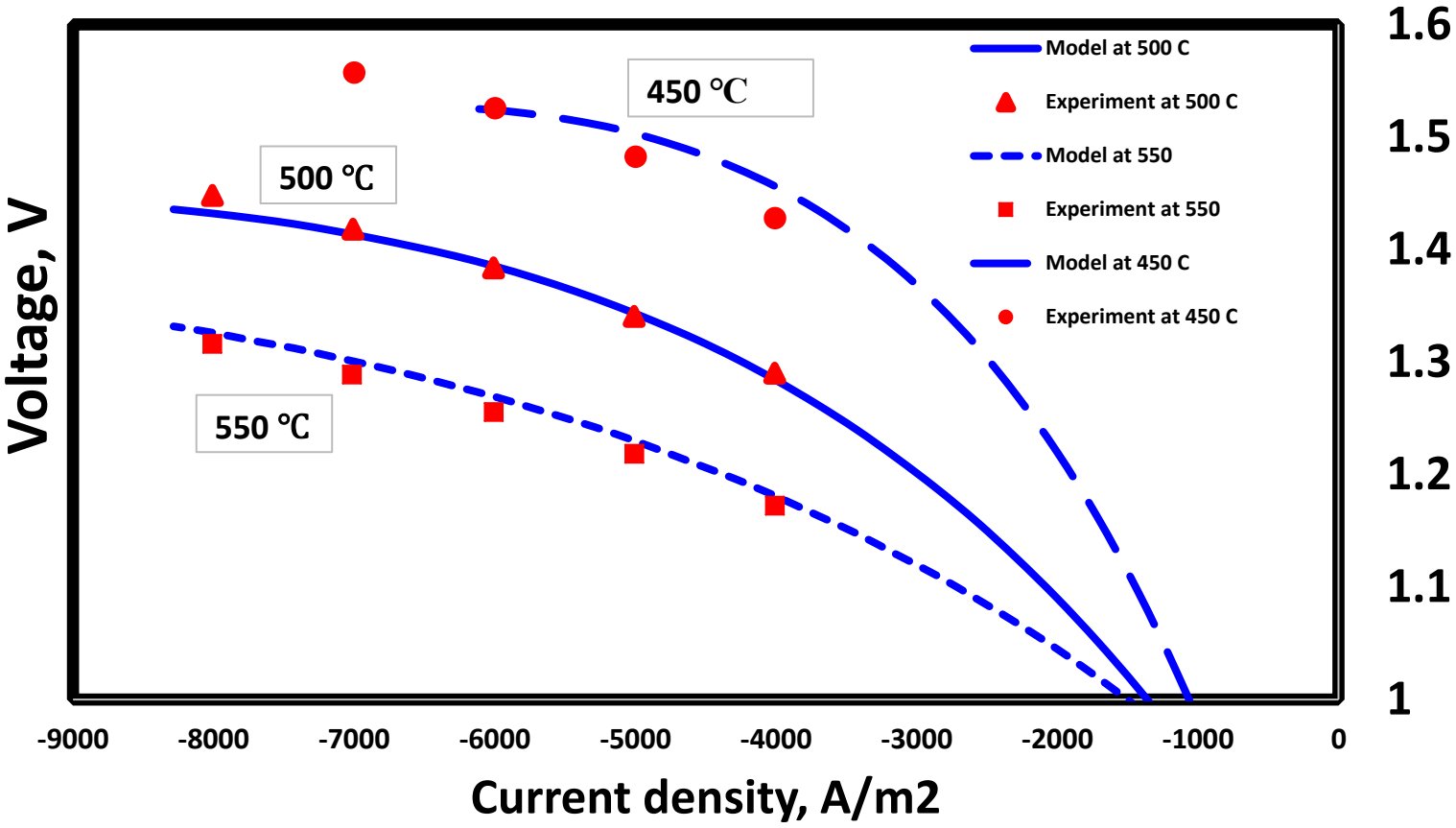

Comprehensive Techno-economic System Modeling of Reversible Methane PCER

In progress

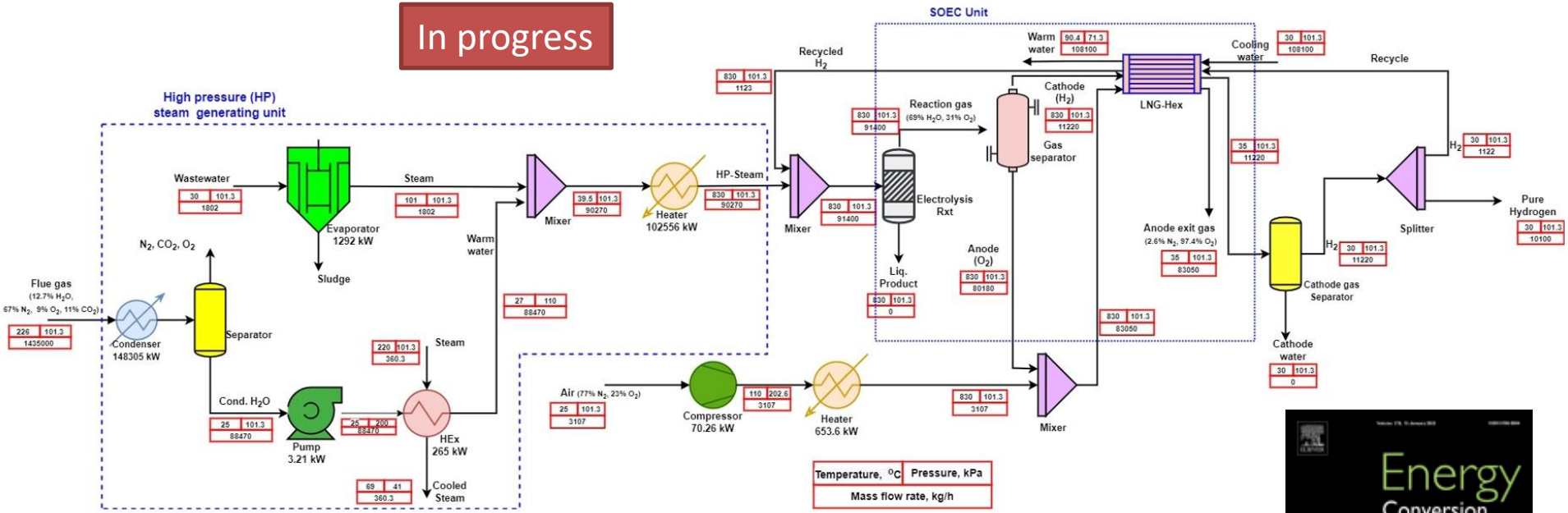

A Novel Hydrogen Economy based on Electrochemical Cells Using Water-Energy Nexus Framework

Proceedings of the ASME 2022 16th International Conference on Energy Sustainability ES2022
July 11-14, 2022, Virtual, Online

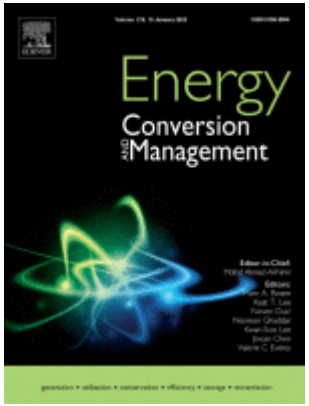

Comprehensive LCA of Reversible Methane PCER

In progress

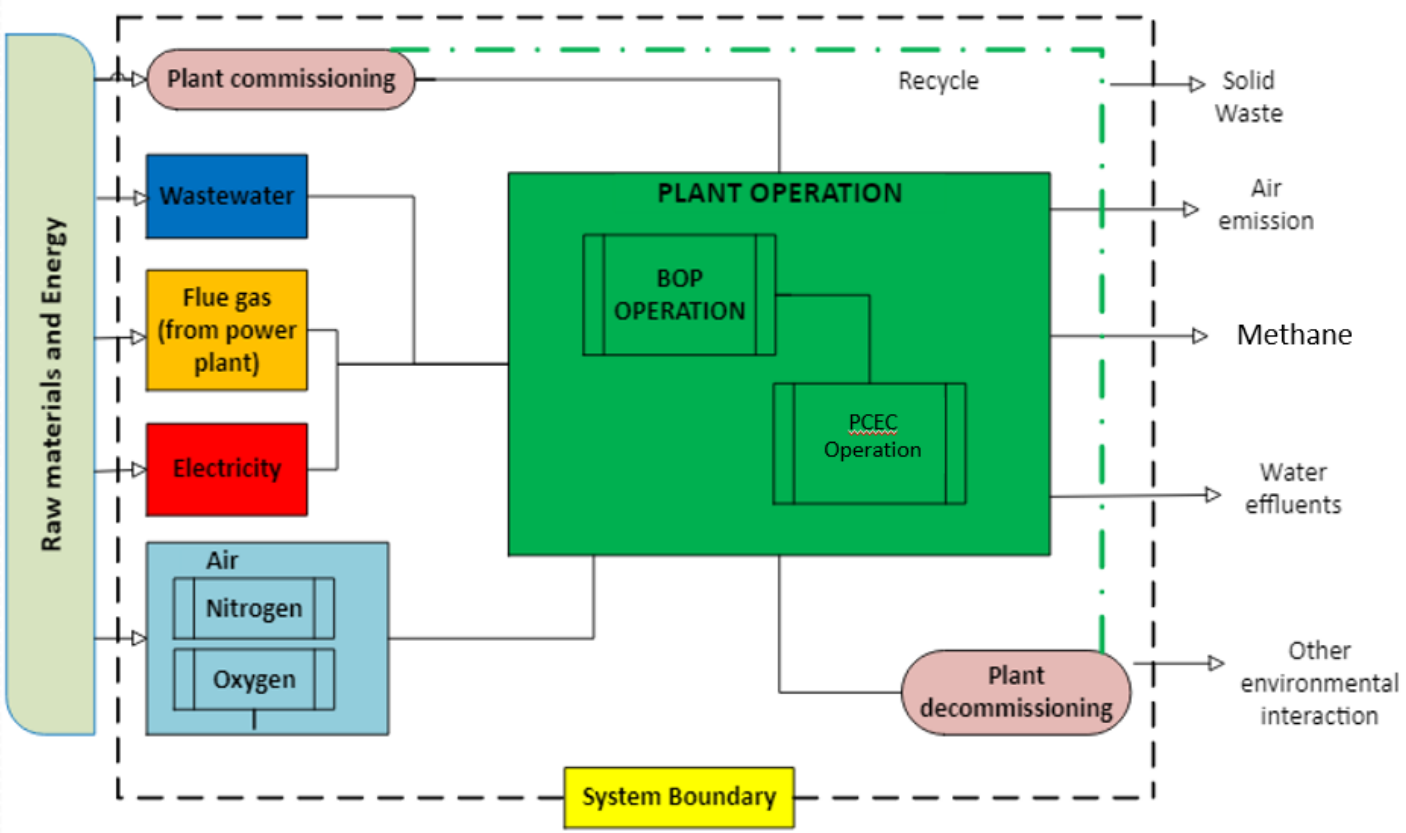

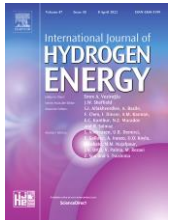

Life Cycles Analysis of a novel integrated Hydrogen production system through water-energy nexus (Under Review)

Levelized cost of hydrogen analysis

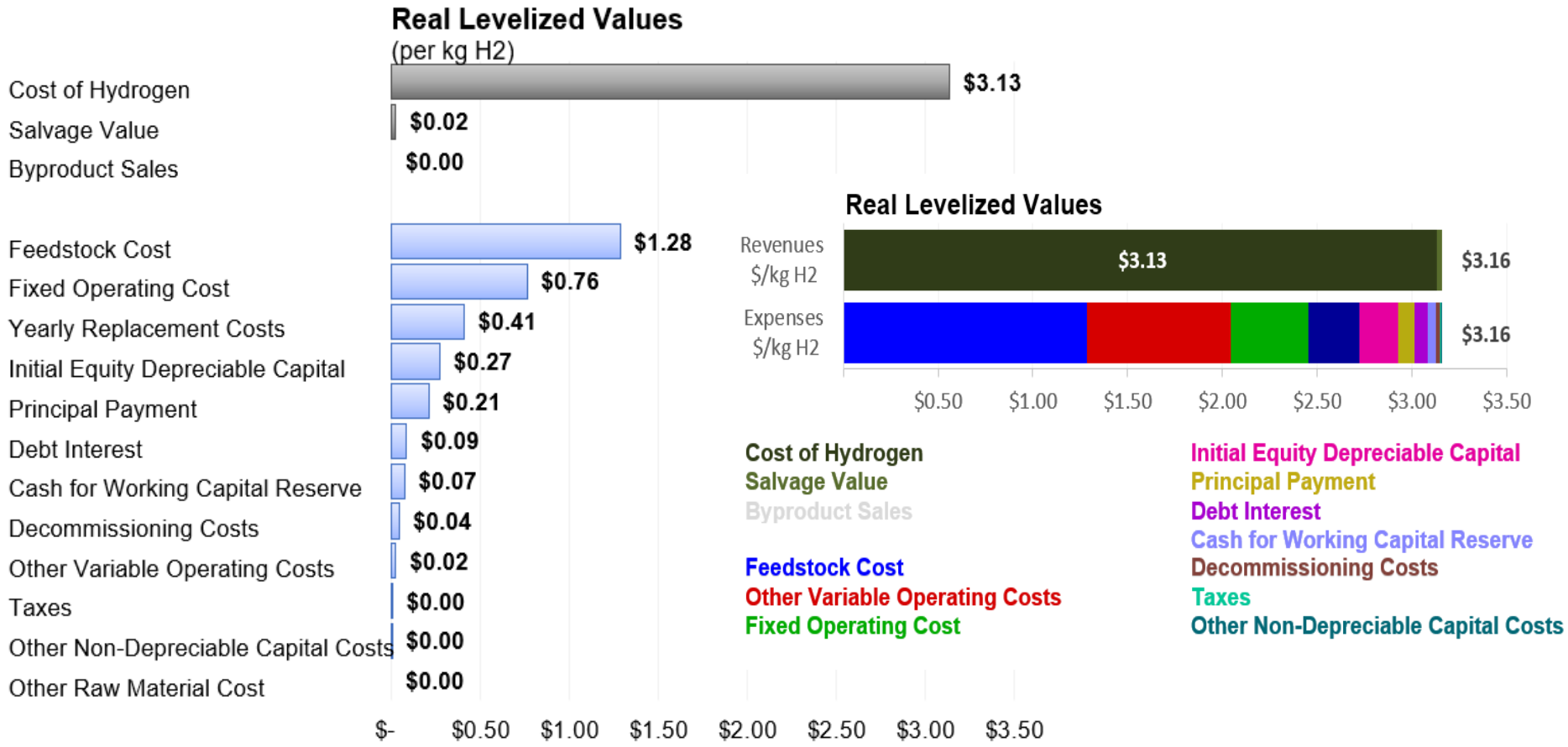

Publications

1-Jolaoso L.A, Asadi J, Duan C, Kazempoor P (2022). A novel green hydrogen production using water-energy nexus framework, Energy Conversion and Management, 276, 116344

2-Liu F; Fang L; Diercks D; Kazempoor P, Duan C, (2022) Rationally designed negative electrode for selective CO2-to-CO conversion in protonic ceramic electrochemical cells; Nano Energy, 102, 107722.

3-Liu F; Park Y; Diercks D; Kazempoor P, Duan C, (2022) Superior catalyst for synthetic natural gas production under mild condition, ACS Applied Materials & Interfaces 14 (11), 13295-13304.

4-Liu F, Diercks D, Kumar P, AbdulJabbar A, Gumeci C, Furuya Y, Dale N, Oku T, Usuda M, Kazempoor P, Fang L, Chen D, Duan C, Lower the operating temperature of protonic ceramic electrochemical cells to <450°C, Nature Energy (Under-review)

5- Liu F, Deng H, Ding H, Kazempoor P, Liu B, and Duan C , Processes-intensified protonic ceramic electrochemical cells for power generation, chemicals production, and greenhouse gas mitigation, Joule (Under-review)

6-Jolaoso L.A, Bello I.T, Ojelade O.A, Kazempoor P, A comprehensive review on Operational and scaling-up barriers of SOEC and mitigation strategies to boost H2 production, International Journal of Hydrogen Energy (under review)

7- Jolaoso L.A, Asadi J, Duan C, Kazempoor P (2022). Life cycles analysis of a novel integrated hydrogen production system through water-energy nexus, International Journal of Hydrogen Energy (Under Review)

Backup Slides

Materials Research Laboratory for Sustainable Energy (MRLSE)

at Kansas State University

Chuanc
Goo
Assist

Tim Taylor Departmen
Kansas S

Please send me an email (cduan@ksu.edu) if you would like to join the group!

We have multiple PhD student and Postdoc open positions.

epresentative Publications

lick on figures below to see or download **publications)**

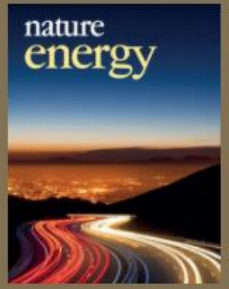

ELECTRODES AND BALANCED REACTIONS

- Anode (steam channel)
- $4H_2O \rightarrow 8H^+ + 2O_2 + 8e^-$

Air (21% O_2 and N_2 balance) is added to this channel

- Cathode (fuel channel)
- $CO_2 + 8H^+ + 8e^- \rightarrow CH_4 + 2H_2O$

Argon is feed to this channel to act as a sweep gas

Overall reaction:

$CO_2 + 4H_2O \rightarrow CH_4 + 2H_2O + 2O_2$

PCEC-GLOBAL CHEMICAL REACTION

- The PCEC global chemical reaction for co-electrolysis of CO2 and H2O are:

- $CO_2 + H_2 \rightarrow CO + H_2O$, $\Delta H = -41 kJ/mol$
- $CO + 3H_2 \rightarrow CH_4 + H_2O$, $\Delta H = -206 kJ/mol$
- $CO_2 + 4H_2 \rightarrow CH_4 + 2H_2O$, $\Delta H = -164 kJ/mol$

For Methanation-at the cathode

- $CO_2 + 8H^+ \; 8e^- \rightarrow CH_4 + 2H_2O$
- $E^0 = \frac{1}{8F}\left(\Delta_f G^0_{CO_2} - \Delta_f G^0_{CH_4} - 2 * \Delta_f G^0_{H_2O}\right)$
- $= \frac{1}{8 * 96487 \frac{C}{mol}} \left(-394.4 - (-50.9) - 2 * (-237.1)\right) \frac{kJ}{mol}$

  $= 0.17$ V

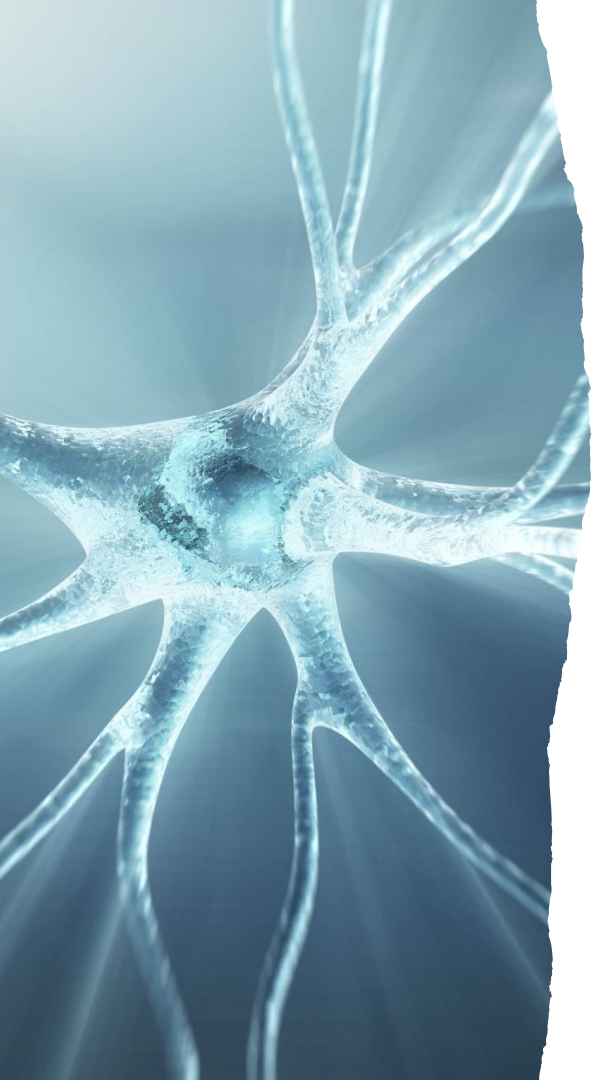

Nernst and cell potential

At the anode

- $E_{O2} = E^0_{O2} - \frac{RT}{nF} ln \left(\frac{P^4_{H2O,an}}{P^2_{O2,an} * P^4_{H2,an}} \right)$

At the cathode,

- $E_{CH4} = E^0_{CH4} - \frac{RT}{nF} ln \left(\frac{P_{CO2,ca} * P^4_{H2,ca}}{P_{CH4,ca} * P^2_{H2O,ca}} \right)$

The open circuit voltage (OCV) is thereby given as:

- $E_{OCV} = \delta(E_{CH4} - E_{O2})$
- $E_{Cell} = E_{OCV}$ + Overpotentials
- δ=f(T) is a balancing factor